THE ANATOMICAL RECORD 302:849–860 (2019)

Sound Generating Structures of the Humpback Dolphin *Sousa plumbea* (Cuvier, 1829) and the Directionality in Dolphin Sounds

GUILHERME FRAINER,[1,2,3]* STEPHANIE PLÖN,[4] NATHALIA B. SERPA,[1,2] IGNACIO B. MORENO,[1,2] AND STEFAN HUGGENBERGER[3]

[1]Programa de Pós-Graduação em Biologia Animal, Departamento de Zoologia, Universidade Federal do Rio Grande do Sul, 91540-000, Porto Alegre, Brazil
[2]Centro de Estudos Costeiros, Limnológicos e Marinhos (CECLIMAR/UFRGS), Campus Litoral Norte, Universidade Federal do Rio Grande do Sul, 95625-000, Imbé, Brazil
[3]Department II of Anatomy, University of Cologne, 50924, Cologne, Germany
[4]African Earth Observation Network (AEON) -Earth Stewardship Science Research Institute (ESSRI), Nelson Mandela University, 6031, Port Elizabeth, South Africa

ABSTRACT

The macroscopic morphology of structures involved in sound generation in the Indian Ocean humpback dolphin (*Sousa plumbea*) were described for the first time using computed tomography imaging and standard gross dissection techniques. The Indian Ocean humpback dolphin may represent a useful comparative model to the bottlenose dolphin (*Tursiops* sp.) to provide insights into the functional anatomy of the sound production in dolphins, since these coastal dolphins exhibit similar body size and share similarities on acoustic behavior. The general arrangement of sound generating structures, that is, air sacs and muscles, was similar in both the bottlenose dolphin and the Indian Ocean humpback dolphin. The main difference between the two species existed in a small left posterior branch of the melon in the Indian Ocean humpback dolphin, which was not found in the bottlenose dolphin and might reflect an adaptation of directionality for high frequency communication sounds as seen in some other delphinids (e.g., *Lagenorhynchus* sp., *Grampus griseus*). Thus, this may be the main reason for the asymmetry of the sound production structures in dolphins. Additionally, the longer rostrum in Indian Ocean humpback dolphins might suggest a more directional echolocation beam compared to the Lahille's bottlenose dolphin. Anat Rec, 302:849–860, 2019. © 2018 Wiley Periodicals, Inc.

Key words: humpback dolphin; sound production; communication; mixed-directionality; echolocation

Grant sponsor: Cetacean Society International; Grant sponsor: Conselho Nacional de Desenvolvimento Científico e Tecnológico; Grant number: 201709/2015-5; Grant sponsor: Coordenação de Aperfeiçoamento de Pessoal de Nível Superior; Grant sponsor: Society for Marine Mammalogy.

*Correspondence to: Guilherme Frainer, Programa de Pós-Graduação em Biologia Animal, Departamento de Zoologia, Universidade Federal do Rio Grande do Sul, 91540-000 Porto Alegre, Brazil. Tel: 55 51 33081267

E-mail: gui.frainer@gmail.com

Received 22 February 2018; Revised 1 June 2018; Accepted 14 July 2018.

DOI: 10.1002/ar.23981
Published online 17 October 2018 in Wiley Online Library (wileyonlinelibrary.com).

Humpback dolphins, genus *Sousa* Grey 1866 (Odontoceti: Delphinidae), are a poorly known genus of cetaceans divided into four species and restricted to tropical and subtropical near-shore coastal waters of the Eastern Atlantic (*S. teutzi*), Indian (*S. plumbea*), and western Pacific (*S. chinensis, S. sahulensis*) Oceans (Ross *et al.,* 1994; Jefferson and Karczmarski, 2001; Parra and Ross, 2009; Rice, 2009; Mendez *et al.,* 2013). They are adapted to live in bay and estuarine habitats, hunting mainly reef-associated, estuarine and demersal fishes (Barros and Cockcroft, 1991; Ross *et al.,* 1994).

Indian Ocean humpback dolphins off South Africa, *S. plumbea*, measure between 97 and 108 cm at birth and reach 280 cm total length in adult males (Ross *et al.,* 1994; Plön *et al.,* 2015), which makes them the largest of all *Sousa* species (Jefferson and Rosenbaum, 2014). Their comparatively small organ weights indicate that humpback dolphins are shallow divers and relative slow moving delphinids (Plön *et al.,* 2012). Although, they are commonly sighted solitary or in groups with a mean size of only seven individuals (Guissamulo and Cockcroft, 2004), recent studies demonstrated a significant decrease in both mean and maximum group size in South African waters (Plön *et al.,* 2015; Koper *et al.,* 2016). The main threat for this species is the accidental entanglement in shark nets (Atkins *et al.,* 2013, 2016), which is the main catalyst for this work as it seems to indicate that these animals cannot sense these nets.

In the present study, the general morphology of the main structures involved in echolocation and social sound generation of the poorly known humpback dolphin is investigated. The detailed descriptions of the main acoustic fat bodies of the Indian Ocean humpback dolphin with additional comparisons to bottlenose dolphin (*Tursiops* sp.) (see Mead, 1975) were useful in interpreting its function, especially regarding social sounds in dolphins.

Sound generation in dolphins takes place in the center of the epicranial (nasal) complex at the MLDB (monkey-lips dorsal bursae) complex, a structure consisting of a lip-like valve of the nasal passage (monkey lips) and accompanying small fat bodies (posterior and anterior dorsal bursae). Air pressure variation in the nasal cavity promotes repeatedly opening and closing movements of these lips, generating a single click each cycle due to vibrations within the associated MLDB complexes (Cranford *et al.,* 1996, 2011). The sound beam seems to be primarily formed by interactions of the MLDB with the skull and the air sacs to form its directional nature (Aroyan *et al.,* 1992; Au *et al.,* 2010; Wei *et al.,* 2017). Accordingly, the sound travels into a large rostral fat body (melon) which acts as an acoustic wave guide by collimating the sound produced by each MLDB complex anteriorly and contributing to narrow the resultant biosonar beam (Wei *et al.,* 2017). In addition, the heterogeneous composition of the fatty melon attenuates the sound to effectively transmit it into the aquatic environment by impedance matching (Harper *et al.,* 2008; McKenna *et al.,* 2012). In this respect, the shape of the melon seems to play a significant role in refining and collimating the sound produced for echolocation (McKenna *et al.,* 2012; Wei *et al.,* 2017).

Besides the echolocation clicks for hunting and navigation/orientation, dolphins commonly produce pulsed calls (e.g., burst pulses and buzzes) (Henderson *et al.,* 2011) and tonal sounds (i.e., whistles) for communication (May-Collado *et al.,* 2007). Pulsed calls are sequences of clicks characterized by the high repetition rate and low interpulse interval and represent the primary mode of communication of some non-whistling odontocetes (e.g., of the genus *Physeter*, *Kogia*, *Platanista*, *Phocoena*, *Cephalorhynchus*) and as common as whistles in dolphins that produce both (Au, 2000). These sounds are associated with several behavioral contexts, such as socializing, aggression, male alliance, affiliative behaviors, play, social feeding, courtship, and others (Herzing, 2000). Dolphin whistles are narrow-band frequency-modulated signals (Au, 2000) and seem to increase in complexity within Delphinoidea due to the evolution of social signals for group cohesion (May-Collado *et al.,* 2007). Both types of communication sounds are known to be made up of harmonics, which may play a role in group navigation due to the mixed-directionality of these sounds (Miller, 2002; Lammers and Au, 2003).

Experimental studies have demonstrated singularities on the sound emission of dolphins in which both echolocation and communication sounds are emitted simultaneously (Ridgway *et al.,* 2015) and with specific source locations: the echolocation signals were produced in the right side of the epicranial complex, while the left side was used for communication sounds, such as whistles and pulsed calls (Madsen *et al.,* 2013). Although, it has been demonstrated that the biosonar beam originates more or less at the center in *T. truncatus* (Moore *et al.,* 2008; Finneran *et al.,* 2014), the source center of the right sound beam may be adjusted by means of the mobility of the nasal plugs by retraction of the nasal plug muscles during vocalizing (Mead, 1975; Heyning and Mead, 1990). Herein, we discuss this asymmetry comparing the biosonar structures *bauplan* of two delphinids with additional comparisons of anatomical and behavioral (acoustic) studies of selected odontocetes from the literature.

MATERIALS AND METHODS

Two Indian Ocean humpback dolphins (Port Elizabeth Museum accession number PEM N5094—female, total length 198.8 cm, condylobasal length 51.50 cm, frozen, carcass condition code 2 (Geraci and Lounsbury, 1993); and PEM N5096—male, total length 262.0 cm, frozen, carcass condition code 3), incidentally caught in shark nets off KwaZulu-Natal (KZN), South Africa, were analyzed at the KwaZulu-Natal Sharks Board facilities, Durban-KZN. It is noteworthy that the Indian Ocean humpback dolphin is a rare and endangered species and obtaining fresh samples from South African waters is not easy due to the climatic conditions. Thus, the scientific collaboration with the KwaZulu-Natal Sharks Board represents a unique opportunity to access the freshest material available. In this context, McKenna *et al*. (2007) have demonstrated that the morphology of the deep soft tissues of the epicranial complex in the dolphin head remain without significant changes postmortem or due to freezing effects (i.e., live, fresh, or thawed). However, superficial soft tissues could exhibit a slight displacement forward due to disarticulation of the head from the body (McKenna *et al.,* 2007). Since the arrangement of the sound emission apparatus appears to have very minor morphological variations at genus level (Mead, 1975; Cranford *et al.,* 1996), we

TABLE 1. List of anatomical abbreviations including the old/usage nomenclature (when applied), the current terminology and the reference used

Abbreviation	Old/usage nomenclature	Current nomenclature	Reference
Bl	Left branch of the melon	*Corpus adiposum nasalis terminalis*	Cranford *et al*. (1996), Huggenberger *et al*. (2014)
Br	Right branch of the melon	*Corpus adiposum nasalis terminalis*	Cranford *et al*. (1996), Huggenberger *et al*. (2014)
Cana	Anterior dorsal bursae	*Corpus adiposum nasalis anterior*	Cranford *et al*. (1996), Huggenberger *et al*. (2014)
Canp	Posterior dorsal bursae	*Corpus adiposum nasalis posterior*	Cranford *et al*. (1996), Huggenberger *et al*. (2014)
melon	Melon	*Corpus adiposum nasalis terminalis*	Mead (1975), Huggenberger *et al*. (2014)
M	Maxillary bone	*Maxilla*	Mead and Fordyce (2009), Nomina Anatomica Veterinaria (2017)
MLDB	Monkey lips dorsal bursae complex	-	Cranford *et al*. (1996)
Mm	-	*Musculus maxillonasolabialis*	Huber (1934), Huggenberger *et al*. (2009)
OI	Premaxillary bone	*Os incisivum*	Mead and Fordyce (2009), Nomina Anatomica Veterinaria (2017)
ON	Nasal bone	*Os nasale*	Mead and Fordyce (2009), Nomina Anatomica Veterinaria (2017)
Snn	Nasofrontal air sacs	*Saccus nasalis nasofrontalis*	Murie (1874), Huggenberger *et al*. (2014)
Snp	Premaxillary air sacs	*Saccus nasalis praemaxillaris*	Murie (1874), Huggenberger *et al*. (2014)
Snv	Vestibular air sacs	*Saccus nasalis vestibularis*	Lawrence and Schevill (1956), Huggenberger *et al*. (2014)
Vnd	Lip of blowhole	*Valva nasalis dorsalis*	Rodionov and Markov (1992), Huggenberger *et al*. (2014)
Vni	Monkey lips	*Valva nasalis intermedia*	Cranford *et al*. (1996), Huggenberger *et al*. (2014)
Vnv	Nasal plugs	*Valva nasalis ventralis*	Cranford *et al*. (1996), Rodionov and Markov (1992)

discuss our findings based on what is known about the sound production in *Sousa* spp.

The analyses of the anatomical topography of the biosonar-related structures were based on a transverse computed tomography scan (CT-scan) of the female´s head (N5094) using Toshiba Aquilion (120 KV, 225 mAs). The head was aligned longitudinally with the bed of the CT-scan and dorsoventrally at 90° to avoid distortions promoted by gravity during scanning. The CT-scan generated a sequence of images (1 mm slice thickness, 0.724 mm pixel edge length) in all three planes (i.e., coronal, sagittal, and axial) that were analyzed using 3D-Slicer (http://slicer.org/). The main biosonar-related components were identified using the segmentation technique (Cranford *et al.,* 2008). In short, images were analyzed and edited voxel by voxel on the three planes accomplished with a threshold assistance tool. Then, a 3D model of each fat and bone structure was generated, and the respective volumes and dimensions were calculated. The size of the brain was characterized by the height of the cranial vault for comparative purposes (Huggenberger *et al.,* 2010). Both heads were dissected, removing tissues layer by layer following the procedure of Schenkkan (1972). Photos of the dorsal view from the female (N5094) were taken to measure and demonstrate the surface area of the air sacs (i.e., vestibular, nasofrontal, and premaxillary) using ImageJ (https://imagej.nih.gov/ij) and Photoshop (www.adobe.com), respectively. The air sacs were collapsed during dissection and, therefore, do not represent the shape of this dynamic structure while *in vivo.* However, the data provided here address a comparative approach with other odontocetes whose air sac morphology has been investigated using gross dissection technique (Schenkkan, 1973).

In addition, one existing CT-scan series (1 mm slice thickness, 0.912 mm pixel edge length) of a male Lahille's bottlenose-dolphin, *Tursiops gephyreus*, (*Grupo de Estudos de Mamíferos Aquáticos do Rio Grande do Sul* accession number GEMARS 1447, total length 248.0 cm, condylobasal length: 51.13 cm, frozen, carcass condition code 2) was used to compare the head morphology of the Indian Ocean humpback dolphin with this well described delphinid (Schenkkan, 1973; Mead, 1975; Rodionov and Markov, 1992; Cranford *et al.,* 1996). Terminology follows Mead (1975) and Huggenberger *et al*. (2014) for soft tissues and Mead and Fordyce (2009), adapted to Nomina Anatomica Veterinaria (2017), for the skull (see the list of abbreviations in Table 1). In this contribution, we assumed the terminology "posterior branch" for all fat bodies between the main body of the melon (connected to it or not) and the dorsal bursae complexes to address a comparative approach.

RESULTS

In general, the epicranial complex of the Indian Ocean humpback dolphin specimens (Figs. 1 and 2) exhibited a similar arrangement to that of other delphinids (see Schenkkan, 1973; Mead, 1975), such as the Lahille's bottlenose dolphin (Fig. 2). However, specific features regarding the position, shape, and asymmetry of the specialized fat bodies in the epicranial complex of the Indian Ocean humpback dolphin were remarkably distinct and will be described in detail.

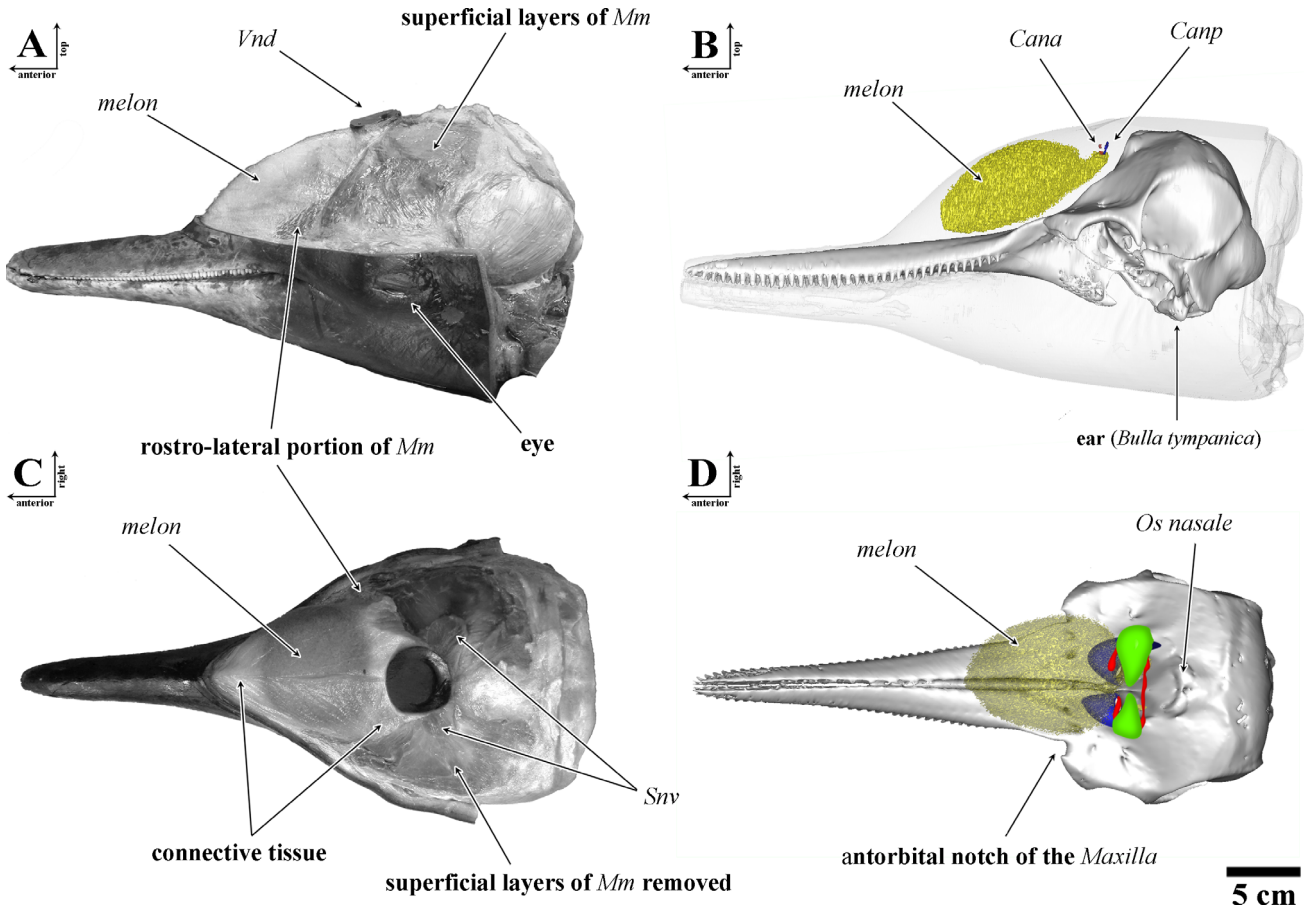

Fig. 1. General topography of the main structures involved in the sound production of a juvenile female (PEM N5094, total length 198.8 cm, condylobasal length 51.5 cm) Indian Ocean humpback dolphin, *Sousa plumbea*. **A**, **C.** Dissected head showing the *Valva nasalis dorsalis* (*Vnd*, lips of the blowhole) and the main body of the *Corpus adiposum nasalis terminalis* (*melon*) and the arrangement of the superficial layers of the *Musculus maxilonasolabialis* (*Mm*) and its rostro-lateral portion in dorsal and lateral view, respectively. **B**, **D**. 3D reconstructions of the specialized fat bodies in the epicranial complex of the same specimen by computed tomography assistance (*melon, Corpus adiposum nasalis terminalis* (yellow); *Cana, Corpus adiposum nasalis anterior* (red); *Canp, Corpus adiposum nasalis posterior* (blue). In **D**, the nasal air sacs were demonstrated at dorsal view (*Saccus nasalis vestibularis*, green; *Saccus nasalis nasofrontalis*, red; *Saccus nasalis praemaxillaris*, blue).

Monkey lips (*Valva nasalis intermedia, Vni*)—These flat lips characterized by small wrinkles on the anterior and posterior side of the epithelium of the nasal passage were placed below the ventral opening of the vestibular air sacs (*Snv*, *Saccus nasalis vestibularis*, see below) and aligned with the dorsal bursae (*Cana*, *Corpus adiposum nasalis anterior* and *Canp*, *Corpus adiposum nasalis posterior*, see below). The wrinkles were surrounded by a thin and light pale pigmentation on both the left- and right-hand side which delimits the structure. On the right *Vni*, the pigmentation was more intense than on the left side (Fig. 3). In both Indian Ocean humpback dolphin specimens, the right *Vni* exhibited deeper and clear wrinkles compared to the left structures where the wrinkles were not clear to the naked eye without shifting the tissue.

Posterior dorsal bursae (*Corpus adiposum nasalis posterior, Canp*)—This pair of small ellipsoid fat bodies were situated posteriorly to each nasal passage and aligned axially 16.03 mm and 14.41 mm in front to the right and left distal-most mesethmoid margin of the nasal bone (*ON*, *Os nasale*), respectively (Fig. 2). The right and left *Canp* were not aligned symmetrically from the mid-sagittal plane, since the left *Canp* was shifted ("skewed") to the right (Figs. 1 and 2). The right *Canp*, instead, was aligned perpendicularly to the mid-sagittal plane and exhibited larger dimensions than the left one (right *Canp* maximum width: 12.84 mm, height: 6.48 mm, axial length: 3.10 mm; left *Canp* max. width: 10.50 mm, height: 3.26 mm, axial length: 2.14 mm). The same size asymmetry between the right and left *Canp* was more evident in the Lahille's bottlenose dolphin (Fig. 2).

Anterior dorsal bursae (*Corpus adiposum nasalis anterior, Cana*)—This second pair of ellipsoid fat bodies were placed anteriorly to each nasal passage just in front of the respective right and left *Canp*. Both *Cana* were aligned to the corresponding *Canp*. The right *Cana* also exhibited larger dimensions than the left one (right *Cana* maximum width: 9.30 mm, height: 3.28 mm, axial length: 2.54 mm; left *Cana* max. width: 6.51 mm, height: 3.33 mm, axial length: 2.33 mm). However, both *Cana* were smaller than the corresponding *Canp* (Fig. 2).

Melon (*Corpus adiposum nasalis terminalis*)—The greatest fat structure in the epicranial complex of the

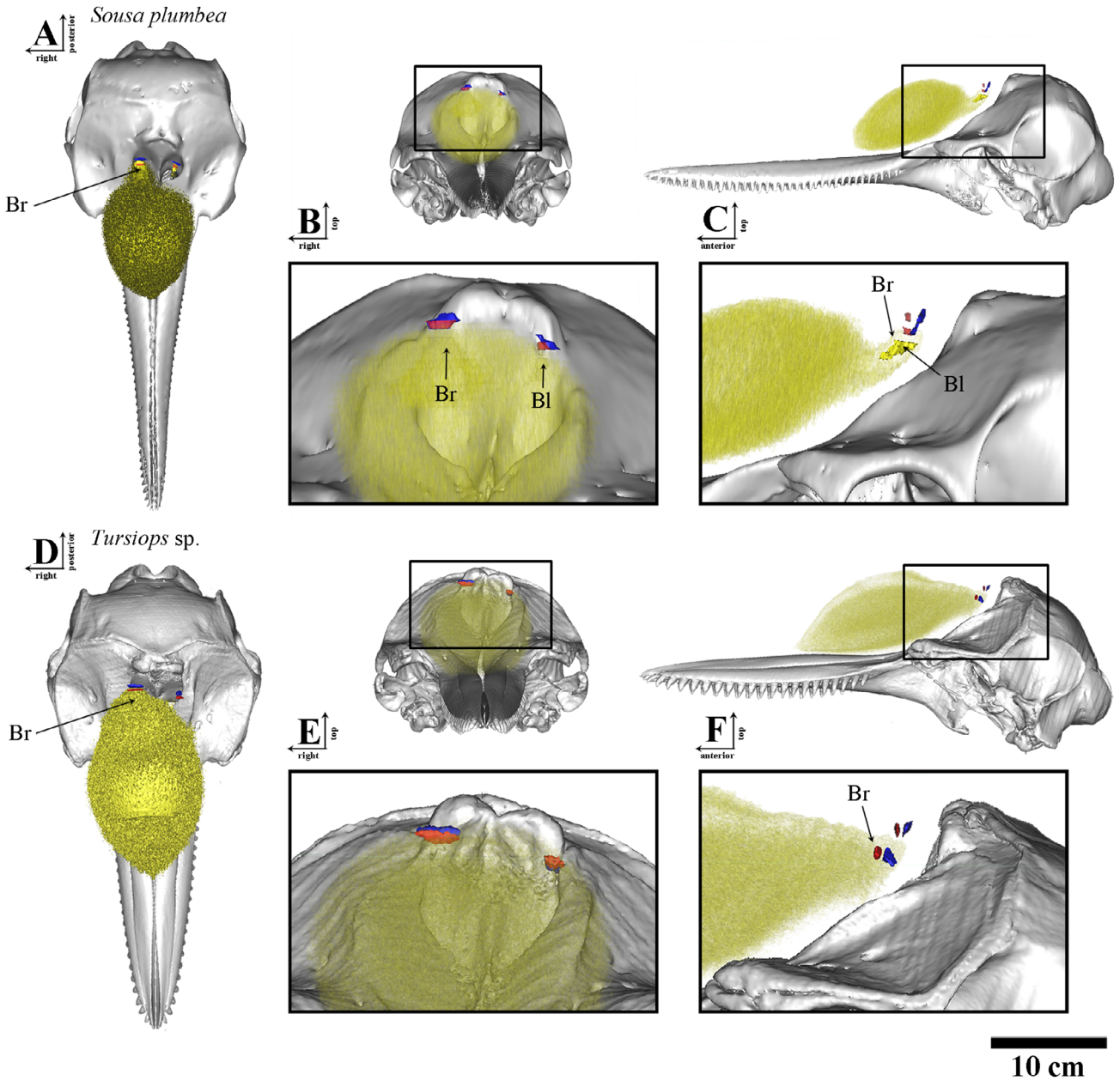

Fig. 2. General topography of the epicranial fat bodies in the Indian Ocean humpback dolphin, *Sousa plumbea* (PEM N5094, total length 198.8 cm, condylobasal length 51.5 cm) (**A–C**) and *Tursiops gephyreus* (GEMARS 1447, total length 248.0 cm, condylobasal length: 51.13 cm) (**D–F**) in dorsal (**A** and **D**), frontal (**B** and **E**), and lateral (**C** and **F**) view (*melon, Corpus adiposum nasalis terminalis* (yellow); left branch of the melon (opaque yellow) *Cana, Corpus adiposum nasalis anterior* (red); *Canp, Corpus adiposum nasalis posterior* (blue); Br, right posterior branch of *melon*; Bl, left posterior branch of the *melon*).

Indian Ocean humpback dolphin resembled the condition found in other delphinids. The anterior portion of the epicranial complex of the Indian Ocean humpback dolphin was nearly totally composed by fat and connective tissues of the *melon*. The rostral musculature of the *Musculus maxilonasolabialis* (*Mm*) was restricted to the lateral borders of the *melon* (Fig. 1). The *melon* originated from both sides of the nasal passage into the nasal plug (*Vnv*, *Valva nasalis ventralis*), where the right and left caudal branches of the *melon* were placed ventral to each *Cana*.

The posterior tip of the right branch of the *melon* in the Indian Ocean humpback dolphin was positioned 2.97 mm and 2.99 mm below to the right *Canp* and *Cana*, respectively (when the nasal passage was collapsed). The width of the right branch of the *melon* at its dorsoposterior portion was 13.90 mm. It extended ventrally 10.52 mm, where it became larger (maximum width at this point: 22.16 mm) and switched its orientation anteriorly, following the skull concavity, until it connected to the main body of the *melon* (maximum width at this point:

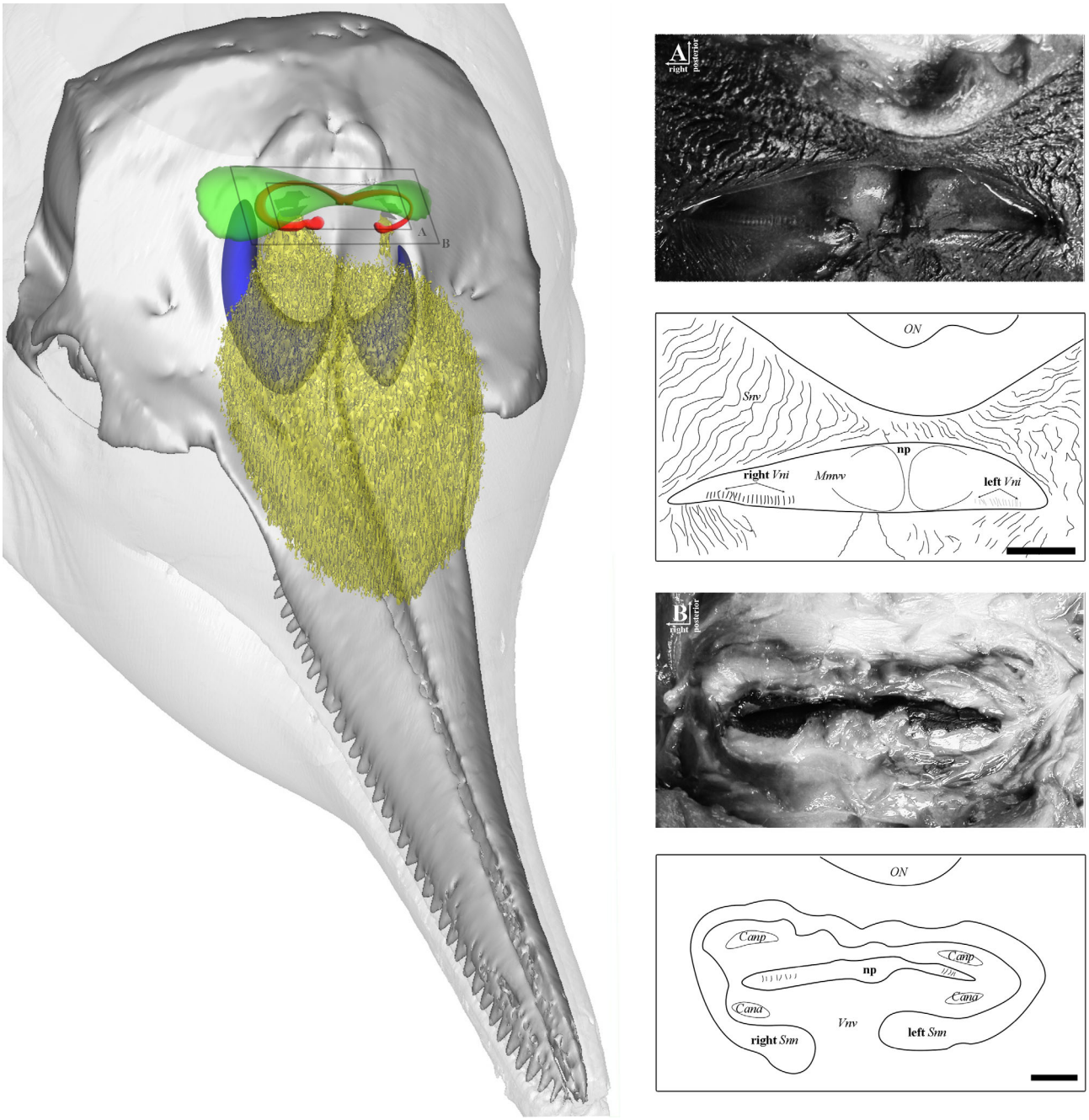

Fig. 3. The general arrangement of the main biosonar-related fat structures (*Corpus adiposum nasalis terminalis*, *melon*, yellow; *Corpus adiposum nasalis posterior*, *Canp*, gray; and *Corpus adiposum nasalis anterior*, *Cana*, gray) of the female Indian Ocean humpback dolphin, *Sousa plumbea* (PEM N5094, total length 198.8 cm, condylobasal length 51.5 cm) relative to the nasal air sacs (schematic representation) (*Saccus nasalis vestibularis, Snv*, green; *Saccus nasalis nasofrontalis*, *Snn*, red; *Saccus nasalis praemaxillaris*, *Snp*, blue). In detail, the nasal passage of the dissected viewed from above at two levels: **A.** Inside the *Snv* showing both right and left-hand side *Valva nasalis intermedia* (*Vni*); and **B.** Below to the *Snv*, showing the (*Snn*) surrounding the nasal passage (np) and the *Canp* and *Cana* into the *Valva nasalis ventralis* (*Vnv*), just in front of the *Os nasale* (*ON*, nasal bone). Scale bars: 1 cm.

45.46 mm; Fig. 2). The length of the right branch of the *melon* (i.e., from its posterior tip to the posteriormost point of the main body of the *melon*) in the Indian Ocean humpback dolphin was 25.60 mm. The left branch of the *melon* was smaller than the right one and did not connect to the main body of the *melon.* Instead, it extended ventrally while entering in the dense connective tissue of the nasal plug. It was positioned 4.33 mm and 3.91 mm ventrally to the left *Canp* and *Cana*, respectively. The width of the left branch of the *melon* at its dorsoposterior

TABLE 2. Morphometric parameters of the specialized fat bodies (*Canp*, *Cana*, and *melon*) of *Sousa plumbea* (PEM 5094, total length 198.8 cm) and *Tursiops gephyreus* (GEMARS 1447, total length 248.0 cm) in mm and relative to the condylobasal length (CBL)

		Sousa		*Tursiops*	
Condylobasal length		515	%CBL	511.3	%CBL
Distance between the *Canp* and the ventrolateral mesethmoid margin of the *ON*	Right	16.03	3.11	18.55	3.63
	Left	14.41	2.80	20.36	3.98
Maximum width of the *Canp*	Right	12.84	2.49	20.22	3.95
	Left	10.50	2.04	10.82	2.12
Height of the *Canp*	Right	6.48	1.26	8.31	1.63
	Left	3.26	0.63	6.30	1.23
Axial length of the *Canp*	Right	3.10	0.60	3.70	0.72
	Left	2.14	0.42	6.39	1.25
Maximum width of the *Cana*	Right	9.30	1.81	20.67	4.04
	Left	6.51	1.26	10.26	2.01
Height of the *Cana*	Right	3.28	0.64	6.77	1.32
	Left	3.33	0.65	5.48	1.07
Axial length of the *Cana*	Right	2.54	0.49	2.36	0.46
	Left	2.33	0.45	3.57	0.70
Distance between the *Canp* and *Cana* complexes and the branches of the *melon*	Right	2.97/2.99	0.57/0.58	1.24/0.73	0.24/0.14
	Left	4.33/3.91	0.84/0.75	-	-
Largest width of the branches of the *melon*	Right	45.46	8.82	69.90	13.67
	Left	4.77	0.93	-	-
Maximum width of the *melon*		100.02	19.42	136.06	26.61
Length of the *melon* with its right branch		159.04	30.88	242.46	47.42
Epicranial complex length	Point to point	160.78	31.21	235.30	46.02
	In parallel	137.08	26.61	223.21	43.66
Elevation angle of the *Canp* and *Cana* complexes	Right	24.35°	-	20.11°	-
	Left	23.45°	-	19.51°	-
Height of the cranial vault		103.5	20.09	128.27	25.08

portion was 4.77 mm. The length of the left branch of the *melon* (i.e., from its posterior tip to the anterior end of this fat body) was 17.67 mm.

The right branch of the *melon* in the Lahille's bottlenose dolphin extended anteriorly, gradually enlarging its diameter to became continuous with the main body of the *melon.* Thus, it was not possible to distinguish the anterior and posterior limits of the right branch of the *melon* in the Lahille's bottlenose dolphin. Additionally, in contrast to the humpback dolphin, there was no evidence of a fat tissue area just anterior to the left *Cana* in the Lahille's bottlenose dolphin. However, a fat protuberance from the axis of the main body of the *melon* on the left side was found (Fig. 2).

The main body of the *melon* of the Indian Ocean humpback dolphin, in dorsal view, was a big triangular fat body with the largest base positioned at 17.19 mm and 19.27 mm in front of both right and left *Cana*, respectively. The largest width of the *melon* was 100.02 mm, just at the line that passed vertically 23.58 mm in front of the antorbital notches of the maxillary bone (*M*, *Maxilla*) in dorsal view. At this point, the *melon* started to taper abruptly from its lateral sides and the top to its anteriormost tip, positioned at the line that passed vertically through the eighth (counted from proximal) tooth of both right and left *M*. The anterior portion of the *melon* was surrounded anteriorly by a connective tissue which gradually lost its fat composition until it reached the skin (Fig. 1). The length of the *melon*, including its right branch (i.e., length between the posterior tip of the *melon* terminus and its anterior tip), was 160.63 mm (32.5% of the condylobasal length). The asymmetry of this structure was evident since the right antorbital notch was almost totally covered by the *melon* in dorsal view, while it covered only the proximal portion of the left antorbital notch (Fig. 1).

The epicranial complex length, that is, distance from the rostroventral tip of the *melon* to the nasal passage between both *Canp* and *Cana* complexes (Huggenberger *et al.,* 2010), of the Indian Ocean humpback dolphin was 194.21 mm from point to point and 167.64 mm in parallel to the sagittal plane. The elevation angle of the *Canp* and *Cana* complexes, determined as the angle between the axis of the skull and the line that passes through the tip of the *melon* to each nasal passage between both MLDB complexes (Huggenberger *et al.,* 2010), was 24.35° on the right and 23.45° on the left side. The association between specialized fat tissues and skull elements in the humpback dolphins was similar to the Lahille's bottlenose dolphin, in contrast to the relative size between the *Canp* and *Cana* complexes which seemed to be more asymmetric in the Lahille's bottlenose dolphin (Table 2).

Vestibular air sacs (*Saccus nasalis vestibularis, Snv*) – The pair of *Snv* were placed just below the blowhole and dorsally covered the posterior portion of the epicranial complex completely. These outpockets of the nasal tract extended laterally (right: 73.2 mm, left: 57.5 mm) from the blowhole forming two rounded and flattened air spaces between the superficial layers of the *Mm* (Fig. 1). In dorsal view, the lateral extension of both *Snv* surpassed the distal borders of the posterior projection of the premaxillary bones (*Os incisivum*, *OI*). The dorsal border of the *Snv* opening was placed posterior to the nasal passage and partially surrounded the vestibulum below the blowhole. The ventral border of the *Snv* opening totally covered the horizontal nasal passage just above the nasal plug muscle (*Musculus maxilonasolabialis valvae ventralis*) and the *Vni.* The size asymmetry between both *Snv*

was evident since the dorsal surface area of the left *Snv* was 13.04 cm^2, about 0.6 times smaller than the right *Snv* (21.27 cm^2). Both *Snv* exhibited a dark coloration of their folded epithelium, in which the folds were oriented in parallel to the axes of the maximum diameter of each *Snv* (Fig. 3).

Nasofrontal air sacs (*Saccus nasalis nasofrontalis, Snn*)—The pair of *Snn* originated on the proximal portion of the posterior walls of each nasal passage, just below the *Snv*. Both sacs surrounded the nasal passage bordering the *Canp* and *Cana* complexes anteriorly, laterally, and posteriorly (Fig. 1). Its epithelium was thin with a dark pigmentation and exhibited small longitudinal folds. The right *Snn* was larger than the left one. Their dorsal surface areas were 6.91 cm^2 and 6.55 cm^2, respectively. The right *Snn* extended 5.43 mm laterally from its medialmost origin, while the left *Snp* extended 4.82 mm laterally. An accessory air sac was not found during the dissections of the two specimens.

Premaxillary air sacs (*Saccus nasalis premaxillaris, Snp*)—As in the bottlenose dolphin, the pair of *Snp* were the largest air sacs in the epicranial complex of the Indian Ocean humpback dolphin (Fig. 1). They were positioned below the *Vnv* and covered 19.59 cm^2 and 9.68 cm^2 of the right and left premaxillary sac fossa of the *OI*, respectively. The maximum width of each sac (i.e., by the line that passed horizontally through the anterior border of each nasal passage) was 5.08 cm for the right and 3.3 cm for the left *Snp*. Thus, the left *Snp* was smaller and narrower compared to the right one, although its anterior tip was placed 0.64 mm in front of the right *Snp* anterior tip. The length of the anterior portion of each *Snp* (i.e., between the anterior border of each nasal passage to the anterior tip of each sac) was 2.65 cm and 3.17 cm for the right and left *Snp*, respectively. Both *Snp* and their opening slits extended laterally around the border of the bony nasal passages. In this way, the right *Snp* opening surrounded the anterior and the lateral border of the naris reaching its posterior limits. The left one extended laterally only half way to the center of the left naris (Fig. 1).

DISCUSSION

The general arrangement of sound generating structures described here for the Indian Ocean humpback dolphin is similar to those described for bottlenose dolphins (*T. gephyreus* and *T. truncatus*, cf. Schenkkan, 1973; Mead, 1975; Rodionov and Markov, 1992; Cranford *et al.,* 1996, this study), that is, the shape of the air sacs as well as the nasal muscles resemble each other in both genera. However, a remarkable difference to bottlenose dolphins exists in the small left posterior branch of the *melon,* which ends anteroventrally to the left bursae complex in the Indian Ocean humpback dolphin.

The shape of the posterior end of the *melon*, which connects the MLDB complex with the melon, attracted some attention in the literature: posterior "rami" or "branches" of the melon were firstly mentioned by Cranford (1988) in the spinner dolphin, *Stenella longirostris*, as small bulbous projections, posterior to the main portion of the melon, which ends on each side of the nasal plug. However, Cranford *et al*. (1996) also described a fat tissue protuberance diverging from the main axis of the melon in the common dolphin, *Delphinus delphis*, as the left branch of the melon, similar to the Lahille's bottlenose dolphin (this study) and the common bottlenose dolphin (*Tursiops truncatus*) (Harper *et al.,* 2008). In this case, the left branch ends posteriorly in the connective tissue and is, thus, not in direct contact to the sound generating structures of the nasal passage (dorsal bursae). Cranford *et al*. (1996) also described "enlarged fatty basins, located between the main body of the melon and (both) MLDB complex(es)" in the Pacific white-sided dolphin (*Lagenorhynchus obliquidens*) and noticed it for the white-beaked dolphin (*Lagenorhynchus albirostris*), Risso's dolphin (*Grampus griseus*), and a neonate northern right whale dolphin (*Lissodelphis borealis*). McKenna *et al*. (2012) used the term "branch" for this *fatty basin* in the Pacific white-sided dolphin. Similar structures were described anterior to the left MLDB complexes in the Franciscana dolphin, *Pontoporia blainvillei*, as "fatty melon branches" (Cranford *et al.,* 1996), but differed from that of the Pacific white-sided dolphin. The right branch connects to the main body of the melon in the Franciscana dolphin, as in most odontocetes, and on the left side is a smaller isolated triangular fat body just anterior to the left anterior dorsal bursa (Cranford *et al.,* 1996; Frainer *et al.,* 2015). Although it seems that this structure was independently acquired in these lineages, it is evident that there is a functional connection between species with this fat body structure connected to the left bursae complex and their sound repertoire:

1. The spinner dolphin is known to produce a high fundamental frequency (~69 kHz) in its whistles compared to other members of the Delphininae subfamily, containing harmonic elements close to 80 kHz (Au *et al.,* 1999b; Lammers and Au, 2003);
2. The Risso's dolphin is known to produce a higher overall frequency in its whistle repertoire compared to other *Globicephala* species and present a high number of harmonics in the barks (ranging from 1 to 28 harmonics) and buzzes (ranging from 20 to 36 harmonics; Corkeron and Van Parijs, 2001);
3. The white-beaked dolphin produces fundamental frequencies of up to 35 kHz with a harmonic element up to 50 kHz, and Rasmussen *et al*. (2006) proposed that whistle production in this species is more directional than seen in the bottlenose dolphin (Rasmussen *et al.,* 2004).
4. Recently, broad band acoustic tags have been able to record high frequency and complex whistles with maximum frequency at 82 kHz for the Franciscana dolphin with up to eight harmonics, a species that ever since was believed to not produce modulated sounds (Cremer *et al.,* 2017).

Humpback dolphins are known to produce broadband clicks for echolocation, ranging from 12 to at least 22 kHz, as well as pulsed calls (i.e., barks, quacks, and grunts) and whistles (Zbinden *et al.,* 1977; Schultz and Corkeron, 1994; Van Parijs and Corkeron, 2001; Weir, 2010; Sims *et al.,* 2012). Schultz and Corkeron (1994) demonstrated that Pacific humpback dolphins produce a higher overall frequency for communication sounds

compared to bottlenose dolphins, and Van Parijs and Corkeron (2001) showed that the barks (i.e., a type of burst-pulses) produced by the Australian humpback dolphin exhibit higher frequencies compared to other delphinids, such as the Atlantic spotted dolphin, *Stenella frontalis*, and the orca, *Orcinus orca* (Ford, 1991; Herzing, 1996), with a number of harmonics ranging from 1 to 22. Sims *et al*. (2012) have recorded barks of the Indo-Pacific humpback dolphin ranging from 4.1 kHz to 24.9 kHz with closely spaced harmonics; in contrast, whistles were simple in structure, with a lower overall frequency compared to barks and a wide spacing between harmonics. However, Weir (2010) have recorded whistles from the Atlantic humpback dolphin with a harmonic structure reaching, at least, 44 kHz.

The acoustic repertoire described for humpback dolphins should be interpreted with caution due to the nature of sampling wild animals (*e.g.,* animal distance/angle from the hydrophone and limitation on recording equipment) and may not represent the whole sound spectrum produced by these animals (Van Parijs and Corkeron, 2001; Weir, 2010). However, the high frequency of burst-pulses and harmonic energy together with the elevated number of harmonics described for burst pulses of humpback dolphins may be a general feature of this genus.

Harmonic social sounds in dolphins are supposed to play a role in group coordination during traveling and hunting since it may provide cues of the moving emitter due to the mixed-directionality of communication sounds (Miller, 2002; Lammers and Au, 2003). Accordingly, higher frequency harmonics are transmitted forward, while lower frequency components are known to be more omnidirectional (Blomqvist and Amundin, 2004). The directionality of the sound produced by dolphins seems to vary between delphinid species (Au *et al.,* 1999a; Rasmussen *et al.,* 2004) and it has been associated with the morphology of the main structures involved in sound emission including the head and rostrum size and the shape of the air sacs (Au *et al.,* 1999a; Song *et al.,* 2016; Wei *et al.,* 2017). Given that fat bodies in the dolphin head are important for absorbing and collimating small wave lengths (i.e., high frequency) and since the heterogeneity of tissue density in the nasal plug may allow for complex timbre across Odontoceti species (Amundin and Andersen, 1983; Cranford *et al.,* 1996; Madsen *et al.,* 2013), we suggest that the asymmetry in the nasal soft tissues found in the Indian Ocean humpback dolphin (i.e., the small left posterior branch of the melon), may indicate one cause among others for adaptation of the high frequency communication sounds reported in this species.

Directionality in dolphin echolocation sounds seems to have evolved to increase the source level (dB) in the forward direction, where click energy presents its elevated center frequency (kHz), thus, increasing the range of target detection and reducing reflection from the periphery (Jensen *et al.,* 2009; Koblitz *et al.,* 2012; Finneran *et al.,* 2014). The directional biosonar beam is formed by interactions with the skull, dense connective tissue surrounding the posterior portion of the melon, air sacs through the right branch of the melon and the melon. (Figs. 1 and 2) (Au *et al.,* 2006; Finneran *et al.,* 2016; Wei *et al.,* 2017). However, dolphins can steer and modify the width of the echolocation beam by changing the frequency emitted (Au *et al.,* 1995; Madsen *et al.,* 2004) and by modulating the shape of the associated soft tissue (*e.g.,* air sacs and melon) through contraction and retraction of the rostral musculature of the *Mm* (Fig. 1) (Moore *et al.,* 2008; Koblitz *et al.,* 2012). Additionally, head movements may allow dolphins to manipulate the sound beam while scanning for prey (Herzing, 1996).

Interestingly, independent toothed whale lineages have evolved convergent (i.e., nonhomologous) specializations for a highly directional echolocation beam production at higher frequencies (i.e., above 120 kHz) and lower source levels compared to other dolphins, the so called NBHF (Narrow-Band High Frequency) species (*e.g.,* pygmy and dwarf sperm whales, *Kogia* spp.; the harbor porpoises, *Phocoena* spp.; the Franciscana dolphins; *Cephalorhynchus* species, *Cephalorhynchus* spp.; and the hourglass dolphin, *Lagenorhynchus cruciger*) (Madsen *et al.,* 2005; Kyhn *et al.,* 2010; Tougaard and Kyhn, 2010). Harbor porpoises, *Cephalorhynchus* species and Franciscana dolphins are small toothed whales inhabiting similar habitats (i.e., coastal waters) and, therefore, the morphological variation found in the biosonar apparatus of these species may reflect the complex factors promoting the directional properties of the sound beam across odontocetes (Wei *et al.,* 2017). However, convergent morphologies in the biosonar apparatus of these species might be useful to interpret meticulous differences between the sound production in the Indian Ocean humpback dolphin and the Lahille's bottlenose dolphin.

Harbor porpoises and *Cephalorhynchus* species are small, non-whistling odontocetes (May-Collado *et al.,* 2007) exhibiting short rostra and a discontinuity between the main body of the melon and the MLDB complex (i.e., the right branch of the melon is absent) which only the dense connective fibers of the nasal plug are remaining and are covered dorsally by the pair of *Snv* (i.e., more developed in the harbor porpoises) (Mead, 1975; Huggenberger *et al.,* 2009). In contrast, the small Franciscana dolphin exhibits the right branch of the melon connected to the main body, while presenting a narrow and long rostrum that, together with the large size of the right *Snv* and the cylindrical melon, may be responsible for the directional properties of the biosonar in this species (Cranford *et al.,* 1996; Huggenberger *et al.,* 2010; Song *et al.,* 2016). Despite the obvious convergence for riverine habitats, the broad-banded clicking Ganges river dolphin (*Platanista gangetica*) exhibits similar morphological adaptations for a directional sound compared to Franciscana dolphins, as this species also presents a long and narrow rostrum and maxillary bony crests acting as sound reflectors above the epicranial complex (Jensen *et al.,* 2013). Harbor porpoises and Franciscana dolphins (and *Cephalorhynchus*, unpublished data by GF) exhibit the MLDB complex aligned in the axial plane with the posterior portion of the melon (Huggenberger *et al.,* 2009; Frainer *et al.,* 2015). This might be related to sound production convergence in these species, since the dorsocaudally position of these structures relative to the melon seems to be a conserved character in delphinids (Fig. 2).

In the present study, we demonstrated that despite the Indian Ocean humpback dolphin exhibiting a continuous melon (i.e., connecting the main body of the melon and the right MLDB complex), it represents a more heterogeneous tissue than the one found in Lahille's bottlenose dolphin. Since there are transverse connective tissue fibers of the nasal plug between the posterior portion of

the right branch of the melon and its main body in the Indian Ocean humpback dolphin (Fig. 2), this could address a distinct sound collimation mechanism. Additionally, the general topography of the biosonar relevant structures differ between both species, which is reflected by the steeper epicranial complex of the Indian Ocean humpback dolphin (i.e., based on the higher values of the elevation angle of the MLDB complex) and its relative longer rostrum compared to the Lahille's bottlenose dolphin. In this way, the data for the Indian Ocean humpback dolphin may challenge previous knowledge that steeper epicranial complexes are related to larger brains (Table 2; Huggenberger *et al.,* 2010). In addition, the longer rostrum in Indian Ocean humpback dolphins might suggest a more directional echolocation beam compared to the Lahille's bottlenose dolphin (Fig. 2; Song *et al.,* 2016).

Coastal NBHF species are not only known to have sophisticated (directional) biosonar systems but also highly negative interaction with fisheries due to accidental entanglement in gill nets (Jefferson and Curry, 1994; Secchi *et al.,* 1997; Iñíguez *et al.,* 2003; Secchi *et al.,* 2004). Despite the fact that mainly calves are captured in these nets, the high mortality of adults may address the higher vulnerability of these particular groups toward gill nets (Reeves *et al.,* 2013). In the same way, the population of Indian Ocean humpback dolphin from the east coast of South Africa has been in decline due to the continued bycatch in shark nets off the KwaZulu-Natal coast (KZN) (Atkins *et al.,* 2013; Plön *et al.,* 2015). Interestingly, the higher bycatch rates are not only due to juveniles being caught, but also males between 2.2 and 2.5 m in length. Another related delphinid, the Indian Ocean bottlenose dolphin (*Tursiops aduncus*), is also threatened by the presence of shark nets, but for this species mostly calves are caught (Cockcroft, 1990; Peddemors, 1999). In the latter species, 30% of all captured calves presented fresh tooth marks indicative of epimeletic behavior (Cockcroft and Sauer, 1990). Thus, lactating females might detect gill nets, but cannot prevent the entanglement of their calves.

Frainer *et al*. (2015) proposed that young individuals of the endangered Franciscana dolphin might be more susceptible to entanglement in fishery gill nets than adults, due to, among other causes, an immature anatomy of biosonar-relevant structures and premature behavior skills related to echolocation. In this respect, the cause of why adolescent male Indian Ocean humpback dolphins exhibit higher bycatch rates is still a matter of speculation. However, we suspect that coastal dolphins with specialized directional echolocation beam are more susceptible to die in gill nets, because they are limited on performing wide range adjustments of their directional properties while pursuing prey or avoiding obstacles (Moore *et al.,* 2008). Franciscana dolphins, for example, do not exhibit rostral musculature of the *Mm*, so the melon axis might be steered mainly by movements of the neck while echolocating. In this way, scanning movements of the head promoted to amplify the inspected area surrounding the animal (Herzing, 1996) might represent a disadvantageous condition for species with a long rostrum, such as Franciscana dolphins and Indian Ocean humpback dolphins. Nevertheless, directional echolocation beams are, theoretically, more restricted to a straightly frontal inspection, while omitting surrounding obstacles. In this way, sudden encounters at short range with a low reflective material (such as the monofilaments of fishing and shark nets) may characterize the bycatch phenomenon of these species specialized in directional echolocation beam generation.

ACKNOWLEDGEMENTS

Our special thanks to Dr. Greg Hofmeyr (Port Elizabeth Museum at Bayworld) and staff of the KwaZulu-Natal sharks board for assistance during dissections and to Dr. Wedderburn-Maxwell (Uhmlanga Hospital, Durban) for his help during CT-image acquisition. We also thank IFAW for financial support to SP. This is a contribution of the Research Group "*Evolução e Biodiversidade de Cetáceos*/CNPq" and an AEON publication no. 178.

LITERATURE CITED

Amundin M, Andersen SH. 1983. Bony nares air pressure and nasal plug muscle activity during click production in the harbour porpoise, *Phocoena phocoena*, and the bottlenosed dolphin, *Tursiops truncatus*. J Exp Biol 105:275–282.

Aroyan JL, Cranford TW, Kent J, Norris KS. 1992. Computer modeling of acoustic beam formation in *Delphinus delphis*. J Acoust Soc Am 92:2539–2545.

Atkins S, Cantor M, Pillay N, Cliff G, Keith M, Parra GJ. 2016. Net loss of endangered humpback dolphins: integrating residency, site fidelity, and bycatch in shark nets. Mar Ecol Prog Ser 555:249–260.

Atkins S, Cliff G, Pillay N. 2013. Humpback dolphin bycatch in the shark nets in KwaZulu-Natal, South Africa. Biol Conserv 159: 442–449.

Au WL. 2000. Hearing in whales and dolphins: an overview. In: Au WL, Richard RF, editors. *Hearing by whales and dolphins*. New York: Springer. p 1–42.

Au WL, Kastelein RA, Benoit-Bird KJ, Cranford TW, McKenna MF. 2006. Acoustic radiation from the head of echolocating harbor porpoises (*Phocoena phocoena*). J Exp Biol 209:2726–2733.

Au WWL, Houser DS, Finneran JJ, Lee W, Talmadge LA, Moore PW. 2010. The acoustic field on the forehead of echolocating Atlantic bottlenose dolphins (*Tursiops truncatus*). J Acoust Soc Am 128:1426–1434.

Au WWL, Kastelein RA, Rippe T, Schooneman NM. 1999a. Transmission beam pattern and echolocation signals of a harbor porpoise (*Phocoena phocoena*). J Acoust Soc Am 106:3699–3705.

Au WWL, Lammers MO, Aubauer R. 1999b. A portable broadband data acquisition system for field studies in bioacoustics. Mar Mamm Sci 15:526–531.

Au WWL, Pawloski JL, Nachtigall PE, Blonz M, Gisner RC. 1995. Echolocation signals and transmission beam pattern of a false killer whale (*Pseudorca crassidens*). J Acoust Soc Am 98:51–59.

Barros NB, Cockcroft VG. 1991. Prey of humpback dolphins (*Sousa plumbea*) stranded in eastern Cape Province. South Africa Aquat Mamm 17:134–136.

Blomqvist C, Amundin M. 2004. An acoustic tag for recording, directional, pulsed ultrasounds aimed at free-swimming Bottlenose dolphins (*Tursiops truncatus*) by conspecifics. Aquat Mamm 30: 345–356.

Cockcroft VG. 1990. Dolphin catches in the Natal shark nets, 1980 to 1988. Afr J Wildl Res 20:44–51.

Cockcroft VG, Sauer W. 1990. Observed and inferred epimeletic (nurturant) behaviour in bottlenose dolphins. Aquat Mamm 16:31–32.

Corkeron PJ, Van Parijs SM. 2001. Vocalizations of eastern Australian Risso's dolphins, *Grampus griseus*. Can J Zool 79: 160–164.

Cranford TW. 1988. The anatomy of acoustic structures in the spinner dolphin forehead as shown by X-ray computed tomography and computer graphics. *Animal Sonar*. Springer, New York. p 67–77.

Cranford TW, Amundin M, Norris KS. 1996. Functional morphology and homology in the odontocete nasal complex: implications for sound generation. J Morphol 228:223–285.

Cranford TW, Elsberry WR, Van Bonn WG, Jeffress JA, Chaplin MS, Blackwood DJ, Carder DA, Kamolnick T, Todd MA, Ridgway SH. 2011. Observation and analysis of sonar signal generation in the bottlenose dolphin (*Tursiops truncatus*): evidence for two sonar sources. J Exp Mar Biol Ecol 407:81–96.

Cranford TW, McKenna MF, Soldevilla MS, Wiggins SM, Goldbogen JA, Shadwick RE, Krysl P, Leger JAS, Hildebrand JA. 2008. Anatomic geometry of sound transmission and reception in Cuvier's beaked whale (*Ziphius cavirostris*). Anat Rec 291:353–378.

Cremer MJ, Holz AC, Bordino P, Wells RS, Simões-Lopes PC. 2017. Social sounds produced by franciscana dolphins, *Pontoporia blainvillei* (Cetartiodactyla, Pontoporiidae). J Acoust Soc Am 141:2047–2054.

Finneran JJ, Branstetter BK, Houser DS, Moore PW, Mulsow J, Martin C, Perisho S. 2014. High-resolution measurement of a bottlenose dolphin's (*Tursiops truncatus*) biosonar transmission beam pattern in the horizontal plane. J Acoust Soc Am 136:2025–2038.

Finneran JJ, Mulsow J, Branstetter BK, Moore P, Houser S. 2016. Nearfield and farfield measurements of dolphin echolocation beam patterns: no evidence of focusing. J Acoust Soc Am 140:1346–1360.

Ford JKB. 1991. Vocal traditions among resident killer whales (*Orcinus orca*) in coastal waters of British Columbia. Can J Zool 69: 1454–1483.

Frainer G, Huggenberger S, Moreno IB. 2015. Postnatal development of franciscana's (*Pontoporia blainvillei*) biosonar relevant structures with potential implications for function, life history, and bycatch. Mar Mamm Sci 31:1193–1212.

Geraci JR, Lounsbury VJ. 1993. *Marine mammals ashore—a field guide for strandings*. Texas: Texas A&M University Sea Grant Publication.

Guissamulo A, Cockcroft VG. 2004. Ecology and population estimates of Indo-Pacific humpback dolphins (*Sousa chinensis*) in Maputo Bay, Mozambique. Aquat Mamm 30:94–102.

Harper C, McLellan W, Rommel S, Gay D, Dillaman R, Pabst D. 2008. Morphology of the melon and its tendinous connections to the facial muscles in bottlenose dolphins (*Tursiops truncatus*). J Morphol 269:820–839.

Henderson EE, Hildebrand JA, Smith MH. 2011. Classification of behavior using vocalizations of Pacific white-sided dolphins (*Lagenorhynchus obliquidens*). J Acoust Soc Am 130:557–567.

Herzing DL. 1996. Vocalizations and associated underwater behavior of free-ranging Atlantic spotted dolphins, *Stenella frontalis* and bottlenose dolphins, *Tursiops truncatus* Aquat Mamm 22:61–80.

Herzing DL. 2000. Acoustics and social behavior of wild dolphins: implications for a sound society. In: Au WL, Richard RF, editors. *Hearing by whales and dolphins*. New York: Springer. p 225–272.

Heyning JE, Mead JG. 1990. Evolution of the nasal anatomy of cetaceans. In: Thomas JA, Kastelein RA, editors. *Sensory abilities of cetaceans*. Boston, MA: Springer. p 67–79.

Huber E. 1934. Anatomical notes on Pinnipedia and Cetacea. Carnegie Inst Wash Publ 447:105–136.

Huggenberger S, André M, Oelschlager HA. 2014. The nose of the sperm whale: overviews of functional design, structural homologies and evolution. J Mar Biol Assoc U K 96:783–806.

Huggenberger S, Rauschmann MA, Vogl TJ, Oelschläger H. 2009. Functional morphology of the nasal complex in the harbor porpoise (*Phocoena phocoena* L.). Anat Rec 292:902–920.

Huggenberger S, Vogl TJ, Oelschläger HHA. 2010. Epicranial complex of the La Plata dolphin (*Pontoporia blainvillei*): topographical and functional implications. Mar Mamm Sci 26:471–481.

Iñíguez MA, Hevia M, Gasparrou C, Tomsin AL, Secchi ER. 2003. Preliminary estimate of incidental mortality of Commerson's dolphins (*Cephalorhynchus commersonii*) in an artisanal setnet fishery in La Angelina Beach and Ria Gallegos, Santa Cruz, Argentina. Lat Am J Aquat Mamm 2:87–94.

Jefferson TA, Curry BE. 1994. A global review of porpoise (Cetacea: Phocoenidae) mortality in gillnets. Biol Conserv 67:167–183.

Jefferson TA, Karczmarski L. 2001. *Sousa chinensis*. Mammal Species 655:1–9.

Jefferson TA, Rosenbaum HC. 2014. Taxonomic revision of the humpback dolphins (*Sousa* spp.), and description of a new species from Australia. Mar Mamm Sci 30:1494–1541.

Jensen FH, Bejder L, Wahlberg M, Madsen PT. 2009. Biosonar adjustments to target range of echolocating bottlenose dolphins (*Tursiops* sp.) in the wild. J Exp Biol 212:1078–1086.

Jensen FH, Rocco A, Mansur RM, Smith BD, Janik VM, Madsen PT. 2013. Clicking in shallow rivers: short-range echolocation of Irrawaddy and Ganges river dolphins in a shallow, acoustically complex habitat. PLoS One 8:e59284.

Koblitz JC, Wahlberg M, Stilz P, Madsen PT, Beedholm K, Schnitzler HU. 2012. Asymmetry and dynamics of a narrow sonar beam in an echolocating harbor porpoise. J Acoust Soc Am 131: 2315–2324.

Koper RP, Karczmarski L, Preez D, Plön S. 2016. Sixteen years later: occurrence, group size, and habitat use of humpback dolphins (*Sousa plumbea*) in Algoa Bay, South Africa. Mar Mamm Sci 32: 490–507.

Kyhn LA, Jensen FH, Beedholm K, Tougaard J, Hansen M, Madsen PT. 2010. Echolocation in sympatric Peale's dolphins (*Lagenorhynchus australis*) and Commerson's dolphins (*Cephalorhynchus commersonii*) producing narrow-band high-frequency clicks. J Exp Biol 213:1940–1949.

Lammers MO, Au WL. 2003. Directionality in the whistles of Hawaiian spinner dolphins (*Stenella longirostris*): a signal feature to cue direction of movement? Mar Mamm Sci 19:249–264.

Lawrence B, Schevill WE. 1956. The functional anatomy of the delphinid nose. Bull Mus Comp Zool 114:103–151.

Madsen P, Carder DA, Bedholm K, Ridgway SH. 2005. Porpoise clicks from a sperm whale nose—convergent evolution of 130 KHz pulses in toothed whale sonars? Bioacoustics 15:195–206.

Madsen PT, Kerr I, Payne R. 2004. Echolocation clicks of two free-ranging, oceanic delphinids with different food preferences: false killer whales *Pseudorca crassidens* and Risso's dolphins *Grampus griseus*. J Exp Biol 207:1811–1823.

Madsen PT, Lammers M, Wisniewska D, Beedholm K. 2013. Nasal sound production in echolocating delphinids (*Tursiops truncatus* and *Pseudorca crassidens*) is dynamic, but unilateral: clicking on the right side and whistling on the left side. J Exp Biol 216: 4091–41102.

May-Collado LJ, Agnarsson I, Wartzok D. 2007. Phylogenetic review of tonal sound production in whales in relation to sociality. BMC Evol Biol 7:136.

McKenna MF, Cranford TW, Berta A, Pyenson ND. 2012. Morphology of the odontocete melon and its implications for acoustic function. Mar Mamm Sci 28:690–713.

McKenna MF, Goldbogen JA, Leger JS, Hildebrand JA, Cranford TW. 2007. Evaluation of postmortem changes in tissue structure in the bottlenose dolphin (*Tursiops truncatus*). Anat Rec 290:1023–1032.

Mead JG. 1975. Anatomy of the external nasal passages and facial complex in the Delphinidae (Mammalia: Cetacea). Smithson Contrib Zool (207):1–35.

Mead JG, Fordyce RE. 2009. The therian skull: a lexicon with emphasis on the odontocetes. Smithson Contrib Zool (627):1–248.

Mendez M, Jefferson TA, Kolokotronis S, Krützen M, Parra GJ, Collins T, Minton G, Baldwin R, Berggren P, Särnblad A. 2013. Integrating multiple lines of evidence to better understand the evolutionary divergence of humpback dolphins along their entire distribution range: a new dolphin species in Australian waters? Mol Ecol 22:5936–5948.

Miller PJ. 2002. Mixed-directionality of killer whale stereotyped calls: a direction of movement cue? Behavioral Ecol Sociobiol 52: 262–270.

Moore PW, Dankiewicz LA, Houser DS. 2008. Beamwidth control and angular target detection in an echolocating bottlenose dolphin (*Tursiops truncatus*). J Acoust Soc Am 124:3324–3332.

Murie J. 1874. On the organization of the caaing whale, Globicephalus melas. Trans Zool Soc London 8:236–302.

Nomina Anatomica Veterinaria. 2017. *International Committee on Veterinary Gross Anatomical Nomenclature*. 6th ed. Columbia, MO: World Association of Veterinary Anatomists.

Parra GJ, Ross G. 2009. The Indo-Pacific humpback dolphin, *Sousa chinensis*. In: Perrin WF, Wursig B, Thewissen JGM, editors. *Encyclopedia of marine mammals*. London: American Press. p 576–581.

Peddemors VM. 1999. Delphinids of southern Africa: a review of their distribution, status and life history. J Cetacean Res Manag 1:157–165.

Plön S, Albrecht KH, Cliff G, Froneman PW. 2012. Organ weights of three dolphin species (*Sousa chinensis*, *Tursiops aduncus* and *Delphinus capensis*) from South Africa: implications for ecological adaptation. J Cetacean Res Manag 12:265–276.

Plön S, Cockcroft VG, Froneman WP. 2015. The natural history and conservation of Indian Ocean humpback dolphins (*Sousa plumbea*) in South African waters. In: Jefferson TA, Curry BE, editors. *Advances in marine biology*. Oxford: Academic Press. p 143–162.

Rasmussen MH, Lammers MO, Beedholm K, Miller LA. 2006. Source levels and harmonic content of whistles in white-beaked dolphins (*Lagenorhynchus albirostris*). J Acoust Soc Am 120:510–517.

Rasmussen MH, Wahlberg M, Miller LA. 2004. Estimated transmission beam pattern of clicks recorded from free-ranging white-beaked dolphins (*Lagenorhynchus albirostris*). J Acoust Soc Am 116:1826–1831.

Reeves RR, McClellan K, Werner TB. 2013. Marine mammal bycatch in gillnet and other entangling net fisheries, 1990 to 2011. Endanger Species Res 20:71–97.

Rice DW. 2009. Classification (Overall). In: Perrin WF, Wursig B, Thewisse JGM, editors. *Encyclopedia of marine mammals*. 2nd ed. Academic Press, United States of America. p 234–238.

Ridgway SH, Dibble DS, Van Alstyne K, Price D. 2015. On doing two things at once: dolphin brain and nose coordinate sonar clicks, buzzes and emotional squeals with social sounds during fish capture. J Exp Biol 218:3987–3995.

Rodionov VA, Markov VI. 1992. Functional anatomy of the nasal system in the bottlenose dolphin. In: Thomas JA, Kastelein RA, Supin AY, editors. *Marine mammal sensory systems*. New York: Plenum Press. p 147–177.

Ross GJB, Heinsohn GE, Cockcroft VG. 1994. Humpback dolphins *Sousa chinensis* (Osbeck, 1,765), *Sousa plumbea* (G. Cuvier, 1829) and *Sousa teuszii* (Kukenthal, 1892). Handbook Mar Mamm 5: 23–42.

Schenkkan EJ. 1972. On the nasal tract complex of *Pontoporia blainvillei* Gervais and d'Orbigny 1844 (Cetacea, Platanistidae). Invest Cetacea 4:83–90.

Schenkkan EJ. 1973. On the comparative anatomy and function of the nasal tract in odontocetes (Mammalia, Cetacea). Bijdr Dierk 2:127–159.

Schultz KW, Corkeron PJ. 1994. Interspecific differences in whistles produced by inshore dolphins in Moreton Bay, Queensland, Australia. Can J Zool 72:1061–1068.

Secchi ER, Kinas PG, Muelbert M. 2004. Incidental catches of franciscana in coastal gillnet fisheries in the Franciscana Management Area III: period 1999-2000. Lat Am J Aquat Mamm 3:61–68.

Secchi ER, Zerbini AN, Bassoi M, Dalla-Rosa L, Moller LM, Rocha-Campos CC. 1997. Mortality of franciscanas, *Pontoporia blainvillei*, in coastal gillnetting in southern Brazil: 1994-1995. Rep Int Whal Commn 47:653–658.

Sims PQ, Vaughn R, Hung SK, Würsig B. 2012. Sounds of Indo-Pacific humpback dolphins (*Sousa chinensis*) in west Hong Kong: a preliminary description. J Acoust Soc Am 131:EL48–EL53.

Song Z, Zhang Y, Wei C, Wang X. 2016. Inducing rostrum interfacial waves by fluid–solid coupling in a Chinese river dolphin (*Lipotes vexillifer*). Phys Rev E 93:012411.

Tougaard J, Kyhn LA. 2010. Echolocation sounds of hourglass dolphins (*Lagenorhynchus cruciger*) are similar to the narrow band high-frequency echolocation sounds of the dolphin genus *Cephalorhynchus*. Mar Mamm Sci 26:239–245.

Van Parijs SM, Corkeron PJ. 2001. Vocalizations and behaviour of Pacific humpback dolphins *Sousa chinensis*. Ethology 107:701–716.

Wei C, Au WWL, Ketten DR, Song Z, Zhang Y. 2017. Biosonar signal propagation in the harbor porpoise's (*Phocoena phocoena*) head: the role of various structures in the formation of the vertical beam. J Acoust Soc Am 141:4179–4187.

Weir CR. 2010. First description of Atlantic humpback dolphin *Sousa teuszii* whistles, recorded off Angola. Bioacoustics 19:211–224.

Zbinden K, Pilleri G, Kraus C, Bernath O. 1977. Observations on the behaviour and underwater sounds of the plumbeous dolphin (*Sousa plumbeous* G. Cuvier 1829) in the Indus Delta region. Invest Cetacea 8:259–286.